Spectrochimica Acta Part A 75 (2010) 183–190

Contents lists available at ScienceDirect

Spectrochimica Acta Part A: Molecular and Biomolecular Spectroscopy

journal homepage: www.elsevier.com/locate/saa

# FT-IR, FT-Raman, *ab initio* and DFT structural and vibrational frequency analysis of 6-aminopenicillanic acid

J. Swaminathan [a], M. Ramalingam [b,*], V. Sethuraman [a], N. Sundaraganesan [c], S. Sebastian [c], M. Kurt [d]

[a] *Department of Chemistry, Periyar Maniammai University, Vallam, Thanjavur – 613403, India*
[b] *CRD, PRIST University, Vallam, Thanjavur – 613403, India*
[c] *Department of Physics (Engg.), Annamalai University, Annamalai Nagar 608002, India*
[d] *Ahi Evran Űniversitesi Fen Edebiyat Fakűltesi Fizik Bölűmű, Aşıkpaşa Kampusű 40100 Kirşehir-Turkiye, Turkey*

ARTICLE INFO

*Article history:*
Received 13 March 2009
Received in revised form
27 September 2009
Accepted 8 October 2009

*Keywords:*
FT-IR
FT-Raman
*ab initio*
DFT
6-Aminopenicillanic acid

ABSTRACT

Quantum mechanical calculations of energies, geometries and vibrational wavenumbers of 6-aminopenicillanic acid were carried out by using *ab initio* HF and density functional theory (DFT/B3LYP) methods with 6-311G(d,p) basis set. The optimized geometrical parameters obtained by HF and DFT calculations are in good agreement with experimental X-ray data. A detailed interpretation of the infrared spectra has also been reported. The theoretical IR and Raman spectrograms have been constructed and compared with the experimental FT-IR and FT-Raman spectra. The differences between the observed and scaled wavenumber values of most of the fundamentals are very small. The thermodynamic parameters have also been computed.

## 1. Introduction

Penicillins are one of the most important classes of antibiotics belonging to the group of β-lactam antibiotics [1]. The discovery of 6-aminopenicillanic acid (6APA) in the year 1957 was an important milestone in the history of clinical medicine since it is the precursor of all semi-synthetic penicillins such as amoxicillin, ampicillin [2] etc., and it has become the world's largest selling β-lactam intermediate. Synthesis of cephalosporins from 6APA has also been reported earlier [3]. The derivatives of 6APA have proved to be remarkably safe drugs which can be administered orally and parentarally to patients of all ages even in the presence of renal and hepatic failure unlike certain other groups of antimicrobial agents such as the aminoglycosides and fluoroquinolones [4].

Spectrometric [5] and colorimetric methods [6] of determination of 6APA have been already reported. A high-performance liquid chromatographic method has been carried out for the estimation of 6APA in amino acid mixtures and human serum by post-column alkaline degradation [7]. There is much information available on $^1$H and $^{13}$C NMR spectroscopy of penicillin derivatives [8,9] and solid-state $^{13}$C NMR chemical shifts of 6APA [10].

Literature survey reveals that to the best of our knowledge, only force field parameterisation for 6APA has been done at HF/6-31G* [11]. The main focus of the present investigation is the study of the molecular structure and vibrational spectra of 6APA completely at HF and DFT levels using 6-311G(d,p) basis set and to identify the various normal modes with greater wavenumber accuracy. The density functional theory calculations are reported [12] to provide accurate vibrational frequencies of organic compounds if the calculated frequencies are scaled to compensate for the approximate treatment of electron correlation for basis set deficiencies and for the anharmonicity.

## 2. Experimental details

The compound 6APA in the solid form was purchased from Sigma–Aldrich Chemical Company (U.S.A.) with a stated purity of 99% and it was used as such without further purification. The spectral measurements were carried out at Central Electro Chemical Research Institute (CECRI) Karaikudi (Tamil Nadu), India. The FT-Raman spectrum of 6APA was recorded using 1064 nm line of Nd: YAG laser as excitation wave length in the region 3500-50 $cm^{-1}$ on a Thermo Electron Corporation model Nexus 670 spectrophotometer equipped with FT-Raman module accessory. The FT-IR spectrum of this compound was recorded in the range of 4000–400 $cm^{-1}$ on Nexus 670 spectrophotometer using KBr

---

* Corresponding author. Tel.: +91 4362 233990.
*E-mail address:* km_ramalingam@yahoo.co.in (M. Ramalingam).

1386-1425/$ – see front matter © 2009 Elsevier B.V. All rights reserved.
doi:10.1016/j.saa.2009.10.010

pellet technique at room temperature with a scanning speed of 30 $cm^{-1}$ $min^{-1}$ and a spectral resolution of 4.0 $cm^{-1}$. The observed experimental FT-IR and FT-Raman spectra and the theoretically predicted IR and Raman spectra at HF and B3LYP levels are shown in Figs. 1a, b, 2a and b.

## 3. Computational details

The entire calculations were performed at Hartree-Fock (HF) and density functional (DFT) levels on a Pentium IV processor personal computer using Gaussian 03W [13] program package, invoking gradient geometry optimization [14]. Initial geometry generated from the standard geometrical parameters was minimized without any constraint on the potential energy surface at Hartree-Fock level adopting the standard 6-311G (d,p) basis set. This geometry was then re-optimized again at DFT level using the same basis set for better description of polar bonds of $NH_2$ and COOH groups. The optimized structural parameters were used for the vibrational frequency calculations at DFT level to characterize all the stationary points as minima. By the use of GAUSSVIEW program [15] vibrational frequency assignments were made with a high degree of accuracy. The total energy distribution (TED) was calculated by using the scaled quantum mechanics (SQM) program [16,17] and the fundamental vibrational modes were characterized by their TED.

### 3.1. Prediction of Raman intensities

The Raman activities ($S_i$) calculated with Gaussian 03W [13] program were converted to relative Raman intensities ($I_i$) using the following relationship derived from the intensity theory of Raman scattering [18,19],

$$I_i = \frac{f(\nu_o - \nu_i)^4 S_i}{\nu_i[1 - \exp(hc\nu_i/k_b T)]}$$

where $\nu_o$ is the exciting frequency in $cm^{-1}$, $\nu_i$ the vibrational wavenumber of the $i^{th}$ normal mode, $h$, $c$ and $k_b$ are the fundamental constants and $f$ is a suitably chosen common normalization factor for all the peak intensities. The simulated FT-Raman spectra plotted from the calculated intensity values using pure Lorentzian band shape with a bandwidth of (FWHM) of 10 $cm^{-1}$ has been shown in Fig. 2a and b.

## 4. Results and discussion

### 4.1. Geometric structure

The numbering system adopted for 6APA in this investigation is shown in Fig. 3. As there are four rotomers, viz., the carboxyl, the amino and the two methyl moieties, the molecule can exist in

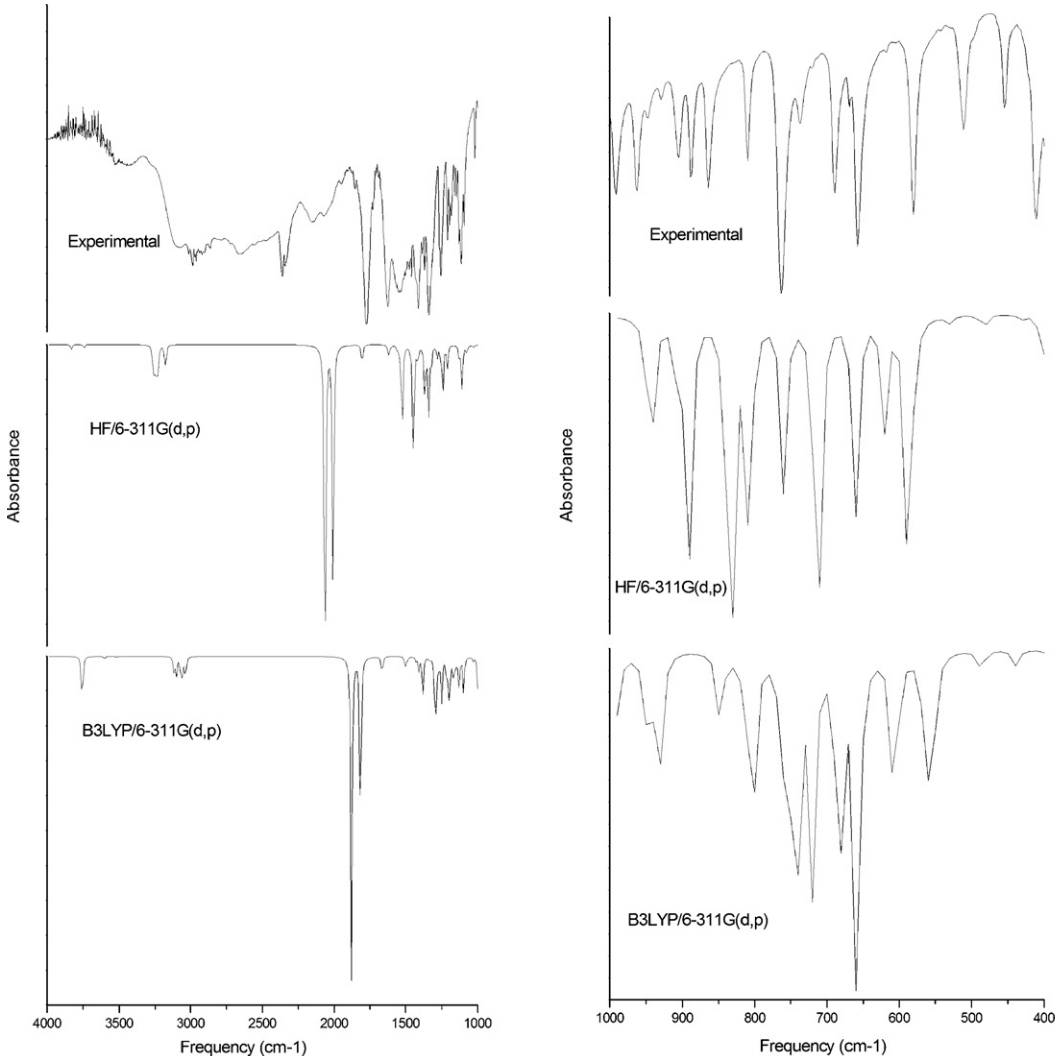

**Fig. 1.** (a) Comparison of FT-IR and theoretical HF and B3LYP spectrum of 6APA; (b) comparison of FT-IR and theoretical HF and B3LYP spectrum of 6APA.

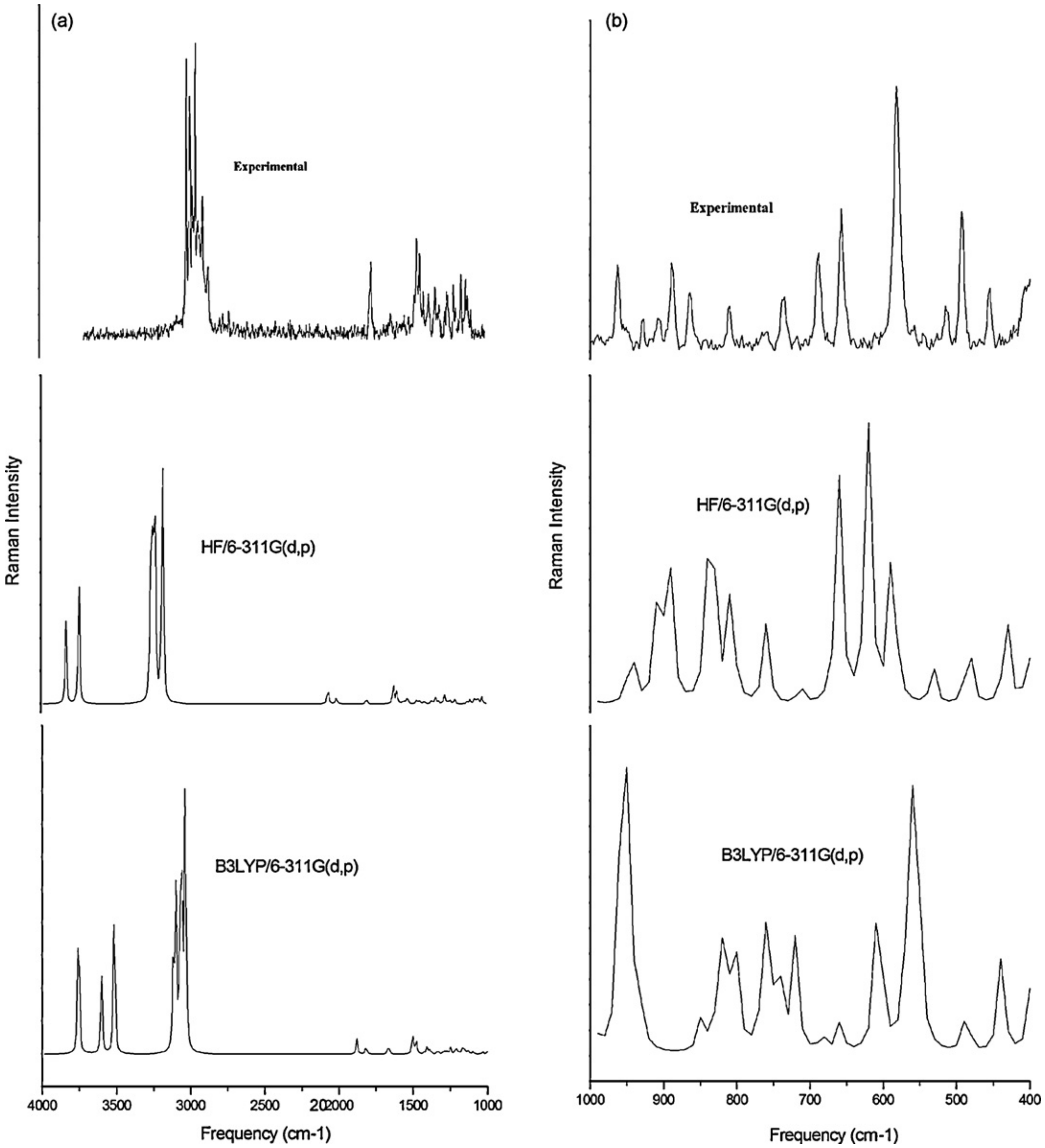

**Fig. 2.** (a) Comparison of FT-Raman and theoretical B3LYP spectrum of 6APA; (b) comparison of FT-Raman and theoretical B3LYP spectrum of 6APA.

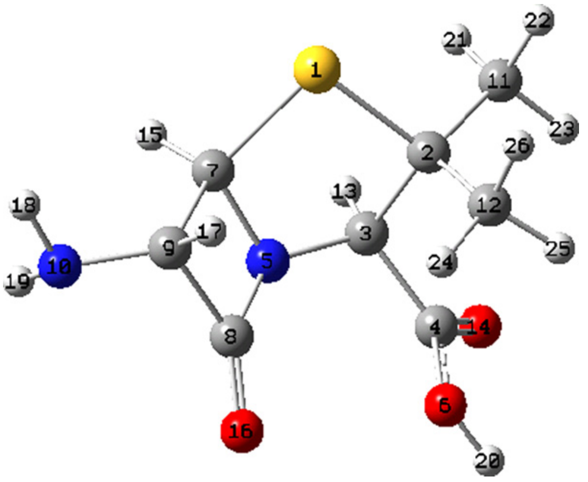

**Fig. 3.** The numbering system adopted for 6APA.

a variety of conformations on the potential energy surface with a number of local minima. Among all the possible minima, the conformation belonging to the lowest minimum was identified through lower level calculation using 3-21G basis set and it was fully optimized at HF and B3LYP using 6-311G(d,p) basis set. The geometrical parameters have been collected in Table 1.

In 6APA there are two ring moieties of which the five membered ring is in envelope shape with C2, S1, C7 and N5 forming the rectangular-facet subtending an angle of ~140° with the triangle-shaped top flap formed by C2, C3 and N5. The azetidin-2-one ring formed by C8, C9, C7 and N5 is fully planar and its angle with the rectangular-faceted five membered ring is ~122°. The conformational analysis reveals that C2–C3, C2–C11 and C2–C12 carbons are at staggered disposition resulting in the less strained envelope shaped five membered ring. The azetidin-2-one ring forces C7–C9 to adopt the eclipsed conformation. The calculated bond lengths on comparison with the experimental values show almost one-to-one correspondence. The Fig. 4 shows the linear relationship between the experimental and calculated bond lengths at HF and B3LYP levels and the regression coefficients are 0.98127, 0.98639 and 0.98964 corresponding to (a), (b) and (c) [20]. The various calculated bond angles and dihedral angles listed in Table 1 are found

**Table 1**
Geometrical and thermodynamic parameters of 6APA.

| Parameter | HF/6-311g(d,p) | B3LYP/6-311g(d,p) | Expt[a] |
|---|---|---|---|
| Interatomic distances | | | |
| S1–C2 | 1.858 | 1.883 | 1.810 |
| C2–C3 | 1.564 | 1.578 | 1.586 |
| C3–N5 | 1.447 | 1.454 | 1.474 |
| N5–C7 | 1.448 | 1.458 | 1.497 |
| C7–S1 | 1.828 | 1.853 | 1.823 |
| C2–C11 | 1.531 | 1.532 | 1.518 |
| C3–C4 | 1.519 | 1.524 | 1.524 |
| C4–O14 | 1.182 | 1.205 | 1.175 |
| N5–C8 | 1.395 | 1.413 | 1.394 |
| C8–O16 | 1.172 | 1.194 | 1.208 |
| C8–C9 | 1.535 | 1.553 | 1.549 |
| C7–C9 | 1.557 | 1.575 | 1.584 |
| C9–N10 | 1.428 | 1.432 | 1.499 |
| Bond angles | | | |
| S1–C2–C3 | 102.6 | 102.8 | |
| C2–C3–N5 | 107.3 | 107.1 | |
| C3–N5–C7 | 114.1 | 114.5 | |
| N5–C7–S1 | 106.5 | 106.4 | |
| C7–S1–C2 | 94.4 | 93.9 | |
| N5–C8–C9 | 91.6 | 91.3 | |
| C8–C9–C7 | 85.0 | 85.1 | |
| C3–C4–O6 | 114.6 | 113.8 | |
| O6–C4–O14 | 123.5 | 123.8 | |
| C3–N5–C8 | 137.2 | 138.2 | |
| N5–C8–O16 | 133.2 | 133.2 | |
| C11–C2–C12 | 110.3 | 110.9 | |
| H18–N10–H19 | 109.3 | 109.3 | |
| Dihedral angles | | | |
| S1–C2–C3–N5 | −36.7 | −36.8 | |
| C2–C3–N5–C7 | 42.3 | 42.7 | |
| C3–N5–C7–S1 | −25.4 | −25.9 | |
| N5–C7–S1–C2 | 1.1 | 1.3 | |
| C7–S1–C2–C3 | 20.0 | 20.0 | |
| C2–C3–C4–O6 | 78.4 | 81.7 | |
| C2–C3–C4–O14 | (99.6 | (95.8 | |
| O14–C4–O6–H20 | (4.6 | (3.7 | |
| C3–C4–O6–H20 | 177.5 | 178.8 | |
| C3–N5–C8–O16 | (48.8 | (47.8 | |
| Thermodynamic parameters | | | |
| Zero point energy (K cal/mol) | 138.7 | 128.4 | |
| Dipole moment | 2.6 | 2.2 | |
| Entropy (cal/mol-K) | | | |
| Total | 115.5 | 119.7 | |
| Translational | 42.0 | 42.0 | |
| Rotational | 31.7 | 31.7 | |
| Vibrational | 42.8 | 46.0 | |

[a] Ref: [21].

to be in satisfactory agreement with the reported standard values. The thermodynamic parameters calculated taking into account the zero-point energy correction have also been collected in Table 1.

### 4.2. *Vibrational spectral analysis*

The experimental assignments of FT-IR and FT-Raman for several vibrational frequencies of 6APA are shown in Table 2 . The theoretically predicted wavenumbers for the various fundamental vibrational modes by *ab initio* HF and density functional methods using 6-311G (d,p) basis set have been collected in Table 2. The title molecule belonging to $C_1$ point group has 72 normal modes of fundamental vibrations. The main focus of the present investigation is the proper assignment of the experimental frequencies to the various vibrational modes of 6APA in corroboration with the scaled down calculated harmonic vibrational frequencies at B3LYP and HF levels using 6-311G(d,p) basis set.

Comparison of the frequencies calculated at HF, B3LYP levels with the experimental values reveals the overestimation of the calculated vibrational modes due to neglect of anharmonicity in real system. Inclusion of electron correlation in density functional theory to a certain extent makes the frequency values smaller in comparison with HF frequency. Reduction in the computed harmonic vibrations, though basis set sensitive is only marginal as observed in the DFT values using 6-311G(d,p) basis set. In our study we have followed two different scaling factors [21] viz. 0.9085 for HF and 0.9668 for B3LYP.

### 4.3. *COOH vibrations*

The most characteristic feature of the carboxylic group is a single band observed usually in the region 1800–1700 $\text{cm}^{-1}$ due to the C=O stretching vibration. In solid state most of the carboxylic acids exist in dimeric form because of the inter molecular hydrogen bonding between two –COOH groups. In such a case two C=O stretching vibrations are expected, one in-phase (symmetric stretching vibration) is Raman active and other one out-of-phase (antisymmetric stretching vibration) is IR active. Esters are characterized by two strong IR absorptions, one due to the C=O stretching vibration in the range 1750–1735 $\text{cm}^{-1}$ and the other due to C–O

**Table 2**

Vibrational wavenumbers and IR intensity obtained for 6APA at HF and B3LYP/6-311G(d,p) [harmonic frequency (cm$^{-1}$), IR intensities (K mmol$^{-1}$)].

| Mode no. | FT-IR | FT-Raman | B3LYP/6-311G(d,p) | | | Vibrational assignments | TED |
|---|---|---|---|---|---|---|---|
| | | | Scaled | IR intensity | Raman intensity | | |
| 1 | | | 27 | 2.760 | 98 | OCO torsion | Γ (O–C–C–C,O–C–C–N)90 |
| 2 | | | 38 | 1.102 | 324 | Four mem. ring torsion | Γ (C–C–C–S,N–C–C–S)70 |
| 3 | | | 47 | 2.669 | 127 | C11–C2–C12 rocking | Γ (C–C–C–S,N–C–C–S)52 |
| 4 | | 150w | 135 | 2.710 | 19 | Five mem. ring breathing | δ (C–C–C,N–C–C)24 + Γ (C–C–C–S,N–C–C–S)44 |
| 5 | | 183w | 158 | 1.082 | 168 | Five mem. ring breathing | δ (C–C–S,C–C–C)16 + Γ (C–C–C–S,N–C–C–O,C–C–C–C)44 |
| 6 | | 196w | 173 | 0.655 | 13 | Five mem. ring torsion | δ (C–C–S,C–C–C)13 + Γ (C–C–C–S,N–C–C–C,C–C–C–C)31 |
| 7 | | 213w | 223 | 3.764 | 36 | N10(H)2 twisting | δ (C–N–C,N–C–C,C–C–C,N–C–O)22 + Γ (C–C–S–C,O–C–N–C,N–C–C–O)13 + Γ (H–N–C–H,H–C–C–C)11 |
| 8 | | | 229 | 4.868 | 20 | N10(H)2 twisting | δ (O–C–C,N–C–C,C–C–C)15 + Γ (C–C–C–S,N–C–C–N,C–C–S–C,N–C–C–O)32 + Γ (H–N–C–C,H–N–C–H)10 |
| 9 | | 229w 244w | 234 | 0.289 | 2.7 | C11(H)3 torsion | Γ (H–C–C–C)60 + Γ (H–C–C–S)28 |
| 10 | | 276w | 255 | 0.676 | 32 | O6–C4–C3 bending | δ (O–C–C)20 + δ (O–C–O,C–C–S,C–C–C)13 + Γ (N–C–C–C,C–N–C–C,C–C–S–C)12 + Γ (H–C–C–S)15 |
| 11 | | | 273 | 11.562 | 73 | N10(H)2 twisting + CH3 twisting | δ (C–C–C,C–C–S)13 + Γ (H–N–C–C)18 + Γ (H–C–C–C)15 |
| 12 | | | 281 | 0.961 | 17 | N10(H)2 twisting + CH3 twisting | Γ (H–C–C–S)20 + Γ (H–C–C–C)52 |
| 13 | | 286w | 297 | 10.805 | 77 | N10(H)2 twisting | Γ (H–N–C–C)36 |
| 14 | | 314w | 326 | 16.838 | 79 | N10(H)2 twisting | ν (C–S)13 + Γ (N–C–C–C,C–C–C–C,O–C–C–C)16 + Γ (H–N–C–C,H–C–C–C)13 |
| 15 | | | 347 | 1.405 | 28 | C11C2C12 bending | ν (C–C)16 + δ (C–C–C)17 + Γ (C–C–S–C,H–C–C–H)17 |
| 16 | | 341w | 357 | 10.496 | 33 | C11C2C12 bending | ν (C–S,C–C)21 + δ (N–C–C,C–C–C)10 |
| 17 | | 399m | 383 | 0.446 | 51 | C2(C3)(C11)(S1) umbrella bending | ν (C–S,C–C,N–C)16 + δ (O–C–C)21 + δ (C–C–C)16 |
| 18 | 411s | | 425 | 3.646 | 44 | S1–C7 stretching + C3–N5–C7 wagging | ν (C–S,C–C)24 + δ (O–C–C,C–C–O)15 + Γ (C–C–C–O,H–C–C–O,H–N–C–C)20 |
| 19 | 454ms | 455m 493ms | 470 | 4.966 | 17 | C2–S1–C7 bending + S1–C7 stretching | ν (C–S,C–C)2O + δ (C–S–C,C–C–O)11 + Γ (S–C–C–C,H–C–C–S,C–C–S–C)16 |
| 20 | 510ms | 514w | 537 | 32.342 | 94 | O6–H bending | ν (C–S)18 + ν (C–C)13 + Γ (H–O–C–C,H–O–C–O)36 |
| 21 | | | 545 | 20.439 | 69 | C3–N5–C7 bending | ν (C–S)15 + ν (C–C)17 + δ (O–C–C,C–C–O)12 + Γ (O–C–C–C,C–C–C–O)14 |
| 22 | 580s | 581vs | 586 | 39.422 | 58 | S1–C2 stretching + O6–H wagging | ν (C–S)22 + δ(O–C–C,O–C–O,H–O–C)12 + δ(O–C–O)18 + Γ (H–O–C–C,H–O–C–O)23 |
| 23 | | | 637 | 77.132 | 8 | O–C–O bending | δ(O–C–C,H–O–C)12 + δ (O–C–O)19 + Γ (H–O–C–C,H–O–C–O)27 |
| 24 | 657s | 657s | 661 | 57.860 | 4 | N10(H)2 wagging | ν (C–S)22 + δ (O–C–C,O–C–O,H–O–C)12 + δ (O–C–O)18 + Γ (H–O–C–C,H–O–C–O)23 |
| 25 | 689ms | 688ms | 697 | 52.867 | 27 | N10(H)2 wagging | ν (C–S,C–C)21 + δ (H–N–C)12 + Γ (H–N–C–C)17 + Γ (H–N–C–H,H–O–C–O)15 |
| 26 | 737w | 735m | 719 | 77.198 | 24 | N10(H)2 wagging + C2–C3 stretching | ν (C–S,C–C)16 + Γ (O–O–C–C,O–C–C–N,O–C–C–C)11 + Γ (H–O–C–O)14 |
| 27 | | | 736 | 22.681 | 29 | N10(H)2 wagging + S1–C7–N5 bending | ν (C–S,C–C,N–C)16 + δ (S–C–C,N–C–C,O–C–C)13 + Γ (C–C–S–C,C–C–C–S,O–C–C–C,H–C–C–S,H–N–C–C)24 |
| 28 | 763vs | | 777 | 49.828 | 31 | N10(H)2 wagging + five and four mem. ring breathing | ν (C–S,C–C,N–C)37 + δ (C–C–N,N–C–C,H–N–C)12 |
| 29 | 810m | 810m | 795 | 1.933 | 24 | N10(H)2 wagging | ν (O–C,C–C,C–N)35 + Γ (O–C–C–N,O–C–C–C,H–O–C–O)23 |
| 30 | 864ms 888m | 864ms 888ms | 819 | 16.952 | 7 | N10(H)2 twisting + S1–C7 stretching | ν (C–S,C–C)19 |
| 31 | | | 900 | 24.443 | 4 | $CH_2$ wagging | ν (C–S,C–C,N–C)58 |
| 32 | | | 913 | 16.403 | 10 | Five and four mem. ring breathing + C12–(H)3 wagging | ν (C–C)30 + ν (O–C)23 + δ (H–C–C)15 |
| 33 | 905m | 907w | 919 | 7.413 | 35 | CH2 of CH3 wagging + C7–C9 stretching | ν (C–C)39 + δ (H–C–C)16 |
| 34 | | 928w | 927 | 0.162 | 26 | C7–C9 stretching + CH2 (CH3) wagging | ν (C–C)37 + δ (H–C–C)30 |
| 35 | 962m | 962ms | 965 | 52.776 | 7 | C9–C8–N5 asym. stretching + CH2 wagging | ν (C–C,N–C,O–C,C–N)46 + δ (O–C–N,C–C–O,H–N–C)17 |
| 36 | 991m | | 998 | 6.528 | 5 | CH2 of CH3 rocking | δ(H–C–C)62 + Γ (H–C–C–H)12 |
| 37 | 1019m | | 1062 | 58.673 | 7.7 | C9–H17 bending | ν (O–C,C–N)32 + Γ (H–C–C–N,H–C–C–H,H–N–C–H)12 |
| 38 | 1093w | | 1092 | 42.489 | 6 | C9–H17 bending + N10(H)2 rocking | ν (C–N,N–C)25 + δ (H–C–C,H–N–C)15 + Γ (H–C–C–S,H–C–C–C)10 |

Table 2 (*Continued* )

| Mode no. | FT-IR | FT-Raman | B3LYP/6-311G(d,p) | | | Vibrational assignments | TED |
|---|---|---|---|---|---|---|---|
| | | | Scaled | IR intensity | Raman intensity | | |
| 39 | | | 1107 | 13.350 | 9 | CH2 of CH3 wagging | δ(H–C–C)37 |
| 40 | 1146w, 1159w | 1158w | 1123 | 14.188 | 10 | C7–H &C9–H wagging + N10(H)2 rocking | ν (N–C)12 + δ (H–C–N,H–N–C,C–C–H)20 + Γ (H–C–S–C,H–C–N–C,H–C–C–H)28 |
| 41 | 1127w | 1128m | 1133 | 24.415 | 12 | C11–C2–C12 asym stretching + CH2 of CH3 rocking | ν (C–C)30 + δ (H–O–C,H–C–C)13 |
| 42 | | | 1157 | 88.471 | 6 | C9–H17 + C7–H15 + O6–H20 bending | ν (O–C,C–C)21 + δ (H–C–C,H–N–C)15 + δ(H–O–C)24 |
| 43 | 1195w | | 1172 | 10.727 | 7 | C9–H17 + C7–H15 + O6–H20 bending | δ(H–C–C,H–N–C,H–O–C,H–C–H)24 + Γ (H–C–C–N,H–C–C–O,H–N–C–H)22 |
| 44 | 1184w | | 1175 | 28.963 | 8 | C2––C3 stretching + C9–H17 bending | ν (O–C,C–C)18 + δ (H–C–C,H–O–C)43 + Γ (H–C–C–C)10 |
| 45 | 1209w | 1210m | 1209 | 65.862 | 13 | C9–N10 stretching + C7–H15 bending | ν (N–C,C–C)38 + δ (H–C–N,H–N–C)11 + Γ (N–C–S–C,C–C–C–H,H–C–C–H,N–C–C–H)22 |
| 46 | | | 1233 | 23.023 | 8 | C7–H15 bending | δ(H–C–S,H–N–C,H–C–N)37 + Γ (N–C–N–C,C–C–C–H,N–C–C–H,H–C–C–H)35 |
| 47 | | | 1251 | 135.254 | 8 | C3–N5 stretching + C3–H + C7–H bending | ν (N–C,C–C)45 |
| 48 | | | 1290 | 5.242 | 8 | C2–C3–H bending | δ(C–C–C)30 + Γ (O–C–C–C,C–N–C–C,O–C–C–O)41 |
| 49 | 1256m | 1255w | 1335 | 55.452 | 2 | N5–C3–H bending + C4–O6–H stretching | ν (C–C)41 + δ (O–C–C,C–C–O,H–O–C)43 |
| 50 | 1339m | 1334w | 1347 | 3.173 | 10 | C3–H bending | δ(C–C–C,N–C–C)23 + Γ (H–C–C–S,O–C–C–H,H–C–C–C,O–C–C–H)46 |
| 51 | | | 1363 | 15.083 | 8 | C11(H)3 + C12(H)3 bending | δ(H–C–C)21 + δ (H–N–C,N–C–H,H–C–H)41 + |
| 52 | 1412w | 1368w 1413w | 1364 | 5.101 | 4 | N10(H)2 twisting + C7–C9–C8 + C9–H bending | δ (H–C–H)24 + δ (H–C–C)16 + δ (C–N–H)18 |
| 53 | 1385w | 1378w | 1384 | 6.475 | 2 | C11(H)3 + C12(H)3 umbrella bending | δ (C–C–H)46 + δ (H–C–H)49 |
| 54 | | | 1429 | 0.863 | 19 | C11(H)2 + C12(H)2 scissoring | δ (H–C–H)45 |
| 55 | | 1439m | 1439 | 3.739 | 4 | C11(H)2 + C12(H)2 scissoring | δ (H–C–H)50 |
| 56 | | | 1450 | 10.932 | 14 | C11(H)2 + C12(H)2 scissoring | δ (H–C–H)48 |
| 57 | 1460w | 1459m | 1454 | 5.170 | 20 | C11(H)2 + C12(H)2 scissoring | δ (H–C–H)48 + Γ (S–C–C–H)13 |
| 58 | 1624m | 1633w | 1610 | 31.764 | 13 | N10(H)2 scissoring | δ (C–N–H)35 + δ (H–N–H)55 |
| 59 | | 1764m | 1756 | 306.175 | 9 | C4=O14 stretching | ν (C=O)86 |
| 60 | 1774ms | | 1816 | 509.424 | 16 | C8=O16 stretching | ν (C=O)87 |
| 61 | | 2902 m | 2931 | 10.519 | 5 | C11(H)3 + C12(H)3 sym. stretching | ν (C–H)100 in methyl part |
| 62 | | 2933ms | 2936 | 25.548 | 103 | C11(H)3 + C12(H)3 sym. stretching | ν (C–H)100 in methyl part |
| 63 | 2962vw | 2952vs | 2956 | 31.044 | 53 | C7–H stretching | ν (C–H)97 |
| 64 | | | 2969 | 9.450 | 20 | C3–H + C9–H stretching | ν (C–H)97 |
| 65 | | 2971s | 2971 | 10.686 | 25 | C9–H stretching | ν (C–H)95 |
| 66 | | | 2993 | 1.589 | 6 | C11(H)3 + C12(H)3 asym. stretching | ν (C–H)100 in methyl part |
| 67 | | | 2999 | 28.049 | 50 | C3–H stretching + C11(H)3 + C12(H)3 asym. stretching | ν (C–H)98 in methyl part |
| 68 | | 3011vs | 3012 | 14.789 | 20 | C3–H stretching + C11(H)3 + asym. stretching | ν (C–H)98 in methyl part |
| 69 | 2984w | 2990v | 3018 | 15.491 | 15 | C12(H)3 asym. stretching | ν (C–H)96 in methyl part |
| 70 | 3651vw | | 3400 | 1.824 | 40 | N10(H)2 sym. stretching | ν (N–H)99 |
| 71 | 3670vw | | 3483 | 3.600 | 20 | N10(H)2 asym. stretching | ν (N–H)100 |
| 72 | 3678w | | 3631 | 85.881 | 30 | O6–H stretching | ν (O–H)100 |

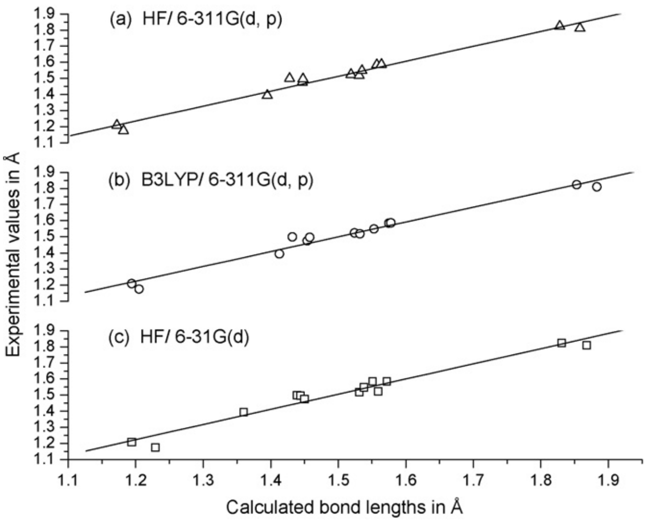

**Fig. 4.** Linear relationship graphs between experimental and calculated bond length values.

stretching near 1200 cm$^{-1}$. Similarly in our case also a medium band observed in FT-IR at 1774 cm$^{-1}$ is assigned to C═O stretching vibration. But the theoretically computed by B3LYP method shows deviations of about 42 cm$^{-1}$ (1816 cm$^{-1}$ mode no. 60) compared to experimental as well as literature value and this deviation may be due to the presence of CH$_3$ group in the adjacent position. Two other characteristic carboxylic group vibrations are C–O stretching and in-plane C–OH bending. They are expected in a wide range of 1450–1150 cm$^{-1}$ depending on whether the acid is monomeric or dimeric. Generally the $\upsilon_{C-O}$ mode appears at lower frequency than C–OH bending vibrations. However, these bands overlap with other bands that are due to the aliphatic chain vibrations causing their undisputed assignment often very difficult. In our present study the frequency observed at 1385 cm$^{-1}$ in FT-IR spectra and 1378 cm$^{-1}$ in FT-Raman are assigned to C–O stretching vibration. The computed values are at 1335 cm$^{-1}$ and 1381 cm$^{-1}$ (mode no. 49) by B3LYP and HF methods respectively for C–O stretching vibration. The HF value shows an excellent agreement with experimental observation. The computed vibrational modes 43 and 42 are assigned to C–OH bending vibrations (1157 and 1172 cm$^{-1}$) which are in satisfactory agreement with the recorded FT-IR at 1195 cm$^{-1}$.

The band due to OH stretching vibrations is much more intense in IR than in Raman spectrum. When carboxylic group forms hydrogen bonding, the result is a broad band centered around 3100–2900 cm$^{-1}$ superimposing C–H stretching vibrations [22,23]. In our study a weak FT-IR band at 3678 cm$^{-1}$ is assigned to OH stretching vibration in addition to the broad band due to the H-bonding observed in the range 3100–2900 cm$^{-1}$. The theoretical calculations predict the wavenumber at 3631 and 3738 cm$^{-1}$ by B3LYP and HF/6-311G(d,p) respectively, the values showing not much deviation from the experimental value of 3678 cm$^{-1}$.

### 4.4. C–H vibrations

In the experimental spectrum, C–H stretching frequencies appear in the range 3100–3000 cm$^{-1}$, the C–H in-plane bending vibrations in the range 1300–1000 cm$^{-1}$ and C–H out-of-plane bending vibrations in the range 1000–750 cm$^{-1}$ [24,25]. The vibrational frequencies at (mode nos. 68, 67 and 63) 3012, 2999 and 2956 cm$^{-1}$ by B3LYP/6-311G(d,p) method assigned to C–H stretching vibrations show good agreement with the recorded spectrum. The FT-IR bands at 1159, 1146, 1093, 1019 cm$^{-1}$ and the FT-Raman band at 1158 cm$^{-1}$ correlate with the B3LYP computed C–H in-plane bending vibrations in the range 1251–1062 cm$^{-1}$ (mode nos. 47–42, 38, 37) coupled with other stretching modes. The C–H out-of-plane bending modes computed by B3LYP and HF methods show consistent agreement with the recorded spectrum.

### 4.5. Methyl group vibrations

In 6APA, there are two CH$_3$ groups attached to the C2 of a five membered heterocyclic ring and we expect a number of stretching and bending vibrations. The asymmetric C–H stretching mode of CH$_3$ group is expected around 2980 cm$^{-1}$ and symmetric one is expected in the region 2870 cm$^{-1}$ [26–29]. In our present study the vibrational frequencies of 3018 and 2969 cm$^{-1}$ (mode nos. 69 and 64) calculated by B3LYP/6-311G(d,p) are assigned to CH$_3$ asymmetric stretching for both the methyl groups present in the molecule. The recorded values of 2984 and 2990 cm$^{-1}$ in FT-IR and FT-Raman spectra respectively are assigned to the same.

The recorded FT-Raman spectrum has medium and weak intensity bands at 2933 and 2902 cm$^{-1}$. They are assigned to CH$_3$ symmetric stretching vibrations for both methyl groups present in the molecule and they do not show much deviation from the computed values of 2936 and 2931 cm$^{-1}$ (mode nos. 62 and 61) by B3LYP/6-311G(d,p) method. The in-plane bending vibrations (scissoring) of the CH3 groups have been identified by the B3LYP method at 1439 and 1429 cm$^{-1}$ (mode no. 55 and 54) and the out-of-plane bending vibration (umbrella) at 1384 cm$^{-1}$ (mode no. 53). They show good agreement with the recorded spectral values observed at 1385 cm$^{-1}$ in FT-IR and 1439 and 1378 cm$^{-1}$ in FT-Raman spectra.

The CH$_3$ rocking vibration has been identified at 998 cm$^{-1}$ by B3LYP method (mode no. 36) and it is in good agreement with the recorded FT-IR spectral value of 991 cm$^{-1}$. The CH3 wagging vibrations computed by B3LYP method are in the range 923–913 cm$^{-1}$ (mode no. 32, 33 and 34) and they show good agreement with the experimentally observed values of 905 cm$^{-1}$ in FT-IR and 907 and 928 cm$^{-1}$ in FT-Raman spectra. Similarly, the calculated CH3 torsional mode of vibration at 234 cm$^{-1}$ (mode no. 9) coincides with the experimental FT-Raman frequencies of 229 and 244 cm$^{-1}$.

### 4.6. C–CH$_3$ vibrations

The C–CH$_3$ stretching vibration is assigned to a weak band observed at 1127 and 1128 cm$^{-1}$ in FT-IR and FT-Raman spectra respectively. The theoretically computed vibrational wavenumber at 1133 cm$^{-1}$ (mode no. 41) is assigned to C–CH$_3$ stretching vibration coupled with CH$_3$ rocking and NH$_2$ rocking vibrations for both the methyl groups present in the molecule. The C–CH$_3$ in-plane and out-of-plane bending vibrations computed by B3LYP/6-311G(d,p) method at 357 and 347 cm$^{-1}$ (mode nos.16 and 15) are consistent with the recorded FT-Raman spectral value of 341 cm$^{-1}$.

### 4.7. NH$_2$ vibrations

The scaled NH$_2$ asymmetric and symmetric stretching modes are at 3483 and 3400 cm$^{-1}$/3480 and 3400 cm$^{-1}$ (mode nos.71 and 70) by B3LYP/HF methods while the experimental values are at 3670 and 3651 cm$^{-1}$ in FT-IR spectrum. In addition, the NH$_2$ group has scissoring, rocking, wagging and torsional modes of vibration. The NH$_2$ scissoring frequency is found at 1610 cm$^{-1}$ by B3LYP and at 1640 cm$^{-1}$ by HF methods and they match with the medium and weak FT-IR and FT-Raman bands observed at 1624 and 1633 cm$^{-1}$. The NH$_2$ wagging mode predicted by B3LYP/6-311G(d,p) method in the region 795–661 cm$^{-1}$ (mode nos. 29–24) is in very good agreement with the observed range of 810–657 cm$^{-1}$ in the FT-IR and FT-Raman spectra.

The $NH_2$ twisting mode is assigned in the FT-Raman spectrum as weak bands at 314 and 286 $cm^{-1}$. It is in consistence with the computed wavenumbers of 326, 297, 281, 273 (mode nos. 14, 13, 12 and 11) by B3LYP method. The rocking mode predicted at 1123 $cm^{-1}$ by B3LYP/6-311G(d,p) method as a coupled vibration of C–C stretching as well as $CH_3$ wagging also shows good agreement with the recorded values of 1159 $cm^{-1}$ and 1158 $cm^{-1}$ in FT-IR and FT-Raman spectra respectively.

### 4.8. Ring vibrations

There are three C–C stretching vibrations in the ring namely C2–C3, C9–C8 and C7–C9 and their corresponding wavenumbers computed by B3LYP method are 1175, 965 and 919 $cm^{-1}$ (mode nos. 44, 35 and 33). The frequencies at 1184 and 962 in FT-IR and 928 $cm^{-1}$ in FT-Raman are assigned to the C–C stretching vibrations.

The identification of C–N stretching mode is a difficult task since mixing up of several vibrational modes is possible in the region. Silverstein [30] assigned C–N stretching vibration in the region 1350–1000 $cm^{-1}$ for amines. By B3LYP method the C–N stretching vibrations calculated at 1251 and 1209 $cm^{-1}$ (mode nos. 47 and 45) for C3–N and C9–N stretching have been shown to be in good agreement with the recorded FT-IR and FT-Raman spectral values in the range of 1256–1201 $cm^{-1}$ and 1255–1210 $cm^{-1}$ respectively. The other vibrations such as ring bending also show consistent agreement with the recorded as well as computed values.

### 4.9. C–S vibrations

In our present study the C–S stretching vibration is observed in both the FT-IR and FT-Raman spectra around 580 $cm^{-1}$. The computed wavenumber for the same mode at 586 $cm^{-1}$ by B3LYP method is in good agreement with the experimental value.

### 4.10. Other molecular properties

The theoretically calculated thermodynamic parameters of 6APA are presented in Table 1. Scale factors have been recommended [31] for an accurate prediction in determining the zero-point vibration energy (ZPVE), and the entropy, $S_{vib}(T)$. The variation in the ZPVE seems to be insignificant. The total energy and the change in the total entropy of 6APA at room temperature are also presented.

## 5. Conclusions

In the present work *ab initio* HF and density functional theory (B3LYP) calculations invoking 6-311G(d,p) basis set on the structure and vibrational spectra have been carried out. The equilibrium geometry computed by HF has shown better results than DFT for both the bond lengths and bond angles. The vibrational analysis by B3LYP method agrees satisfactorily with the experimental results. On the basis of agreement between the calculated and experimental results, assignments of all the fundamental vibrational modes of 6APA have been made for the first time in this investigation. Therefore, the assignments proposed at higher level of theory with higher basis set with only reasonable deviations from the experimental values seem to be correct.

## References

[1] R.E. Kirk, D.F. Othmer, Encyclopedia of Chemical Technology, vol. II, 3rd ed., John Wiley and Sons, New York, NY, 1984, p. 871.
[2] M.B. Diender, A.J.J. Straathof, T. vander Does, C. Ras, J.J. Heijnen, Biotechnol. Bioeng. 98 (4) (2002) 395.
[3] T. Fekner, J.E. Baldwin, R.M. Adlington, T.W. Jones, C. Keith Prout, C.J. Schofield, Tetrahedron 56 (2000) 6053.
[4] G.N. Rolinson, A.M. Geddes, Int. J. Antimicrob. Agents 29 (1) (2007) 3.
[5] N.T. Yatsimirskaya, I.N. Sosnovskaya, A.K. Yatsimirsky, Anal. Biochem. 229 (2) (1995) 249.
[6] J.M. Kornfeld, Anal. Biochem. 86 (1) (1978) 118.
[7] J. Haginaka, J. Wakai, Anal. Biochem. 158 (1) (1986) 146.
[8] W.L. Wilson, H.W. Avdovich, D.W. Hughes, J. Assoc. Off. Anal. Chem. 57 (1974) 1300.
[9] R. Nagarajan, L.D. Boeck, M. Gorman, R.L. Hamill, C.E. Higgens, M.M. Hoehn, W.M. Stark, J.G. Whitney, J. Am. Chem. Soc. 93 (1971) 2308.
[10] M.R.M.P. Aguiar, S.M.C. Menezes, A.L. Gemal, R.A.S. San Gil, Solid State Nucl. Mag. 4 (3) (1995) 179.
[11] O.V. Stroganov, G.G. Chilov, V.K. ŠVedas, J. Mol. Struct. (THEOCHEM) 631 (1–3) (2003) 117.
[12] M. Ramalingam, M. Jaccob, J. Swaminathan, P. Venuvanalingam, N. Sundaraganesan, Spectrochim. Acta 71A (2008) 996.
[13] M.J. Frisch, G.W. Trucks, H.B. Schlegel, G.E. Scuseria, M.A. Robb, J.R. Cheeseman, J.A. Montgomery Jr., T. Vreven, K.N. Kudin, J.C. Burant, J.M. Millam, S.S. Iyengar, J. Tomasi, V. Barone, B. Mennucci, M. Cossi, G. Scalmani, N. Rega, G.A. Petersson, H. Nakatsuji, M. Hada, M. Ehara, K. Toyota, R. Fukuda, J. Hasegawa, M. Ishida, T. Nakajima, Y. Honda, O. Kitao, H. Nakai, M. Klene, X. Li, J.E. Knox, H.P. Hratchian, J.B. Cross, C. Adamo, J. Jaramillo, R. Gomperts, R.E. Stratmann, O. Yazyev, A.J. Austin, R. Cammi, C. Pomelli, J.W. Ochterski, P.Y. Ayala, K. Morokuma, G.A. Voth, P. Salvador, J.J. Dannenberg, V.G. Zakrzewski, S. Dapprich, A.D. Daniels, M.C. Strain, O. Farkas, D.K. Malick, A.D. Rabuck, K. Raghavachari, J.B. Foresman, J.V. Ortiz, Q. Cui, A.G. Baboul, S. Clifford, J. Cioslowski, B.B. Stefanov, G. Liu, A. Liashenko, P. Piskorz, I. Komaromi, R.L. Martin, D.J. Fox, T. Keith, M.A. Al-Laham, C.Y. Peng, A. Nanayakkara, M. Challacombe, P.M.W. Gill, B. Johnson, W. Chen, M.W. Wong, C. Gonzalez, J.A. Pople, Gaussian 03, Revision B.03, Gaussian Inc., Pittsburgh, PA, 2003.
[14] H.B. Schlegel, J. Comput. Chem. 3 (1982) 214.
[15] A. Frisch, A.B. Nielson, A.J. Holder, GAUSSVIEW User Manual, Gaussian Inc., Pittsburgh, PA, 2000.
[16] J. Baker, A.A. Jarzccki, P. Pulay, J. Phys. Chem. 102A (1998) 1412.
[17] P. Pulay, J. Baker, K. Wolinski, Chem. Phys. Letts. 358 (2002) 354.
[18] G. Keresztury, S. Holly, J. Varga, G. Besenyei, A.Y. Wang, J.R. Durig, Spectrochim. Acta 49A (1993) 200.
[19] G. Keresztury, in: J.M. Chalmers, P.R. Griffith (Eds.), Raman Spectroscopy: Theory in Handbook of Vibrational spectroscopy, vol. 1, John Wiley & Sons Ltd., New York, 2002.
[20] A.P. Scott, L. Radom, J. Phys. Chem. 100 (1996) 16502.
[21] Z. Galdecki, M. Werfel, Acta Crystallogr. Sect. A 34 (1978) S90.
[22] M. Samsonowicz, T. Hrynoszkiewiez, R. Swislocka, E. Regulska, W. Lewandowski, J. Mol. Struct. 744 (2005) 345.
[23] M. Baranska, K. Chruszez, B. Boduszek, L.M. Proiewicz, Vib. Spectrosc. 31 (2003) 295.
[24] G. Varsanyi, Assignments of Vibrational Spectra of 700 Benzene Derivatives, Wiley, New York, 1974.
[25] J. Swaminathan, M. Ramalingam, N. Sundaraganesan, Spectrochim. Acta 71A (2009) 1176.
[26] D.A. Kleinman, Phys. Rev. 126 (1962) 1977.
[27] B. Smith, Infrared Spectral Interpretation: A Systematic Approach, CRC Press, Washington, DC, 1999.
[28] J. Swaminathan, M. Ramalingam, V. Sethuraman, N. Sundaraganesan, S. Sebastian, Spectrochim. Acta 73A (2009) 593.
[29] G. Socrates, Infrared Characteristic Frequencies, Wiley Inter Science Publication, New York, 1990.
[30] M. Silverstein, G.C. Basseler, C. Morill, Spectrometric Identification of Organic Compounds, Wiley, New York, 1981.
[31] J. Annama, P. Daizy, K.I. Abdullah, G. Keresztury, S. Devanarayanar, J. Raman Spectrosc. 31 (2000) 1067.